

# Two-dimensional rod theory for approximate analysis of building structures

Hideo Takabatake\*

*Department of Architecture, Kanazawa Institute of Technology, 7-1 Ohgigaoka  
Nonoichi Ishikawa 921-8501, Japan*

*Institute of Disaster and Environmental Science, 3-1 Yatsukaho, Hakusan, Ishikawa Prefecture, 924-0838, Japan*

*(Received December 29, 2009, Accepted February 6, 2010)*

**Abstract.** It has been known that one-dimensional rod theory is very effective as a simplified analytical approach to large scale or complicated structures such as high-rise buildings, in preliminary design stages. It replaces an original structure by a one-dimensional rod which has an equivalent stiffness in terms of global properties. If the structure is composed of distinct constituents of different stiffness such as coupled walls with opening, structural behavior is significantly governed by the local variation of stiffness. This paper proposes an extended version of the rod theory which accounts for the two-dimensional local variation of structural stiffness; viz, variation in the transverse direction as well as longitudinal stiffness distribution. The governing equation for the two-dimensional rod theory is formulated from Hamilton's principle by making use of a displacement function which satisfies continuity conditions across the boundary between the distinct structural components in the transverse direction. Validity of the proposed theory is confirmed by comparison with numerical results of computational tools in the cases of static, free vibration and forced vibration problems for various structures.

**keywords:** simplified analytical method; extended rod theory; two-dimensional stiffness of structures; preliminary design for buildings; dynamic analysis; shear wall with opening.

---

## 1. Introduction

In order to carry out approximate analysis for a large scale complicated structure such as a high-rise building in the preliminary design stages, the use of equivalent rod theory is very effective. Rutenberg (1975), Smith and Coull(1991), Tarjan and Kollar(2004) presented approximate calculations based on the continuum method, in which the building structure stiffened by an arbitrary combination of lateral load-resisting subsystems, such as shear walls, frames, coupled shear walls, and cores, are replaced by a continuum beam. Georgoussis(2006) proposed to assess frequencies of common structural bents including the effect of axial deformation in the column members for symmetrical buildings by means of a simple shear-flexure model based on the continuum approach. Tarian and Kollar(2004) presented the stiffnesses of the replacement sandwich beam of the stiffening system of building structures.

Takabatake *et al.*(1993a,b, 1995, 1996, 2001, 2005, 2006) developed a simple but accurate rod theory which takes account of longitudinal, bending, and transverse shear deformation, as well as

---

\*Professor, Director, E-mail: [hideo@neptune.kanazawa-it.ac.jp](mailto:hideo@neptune.kanazawa-it.ac.jp)

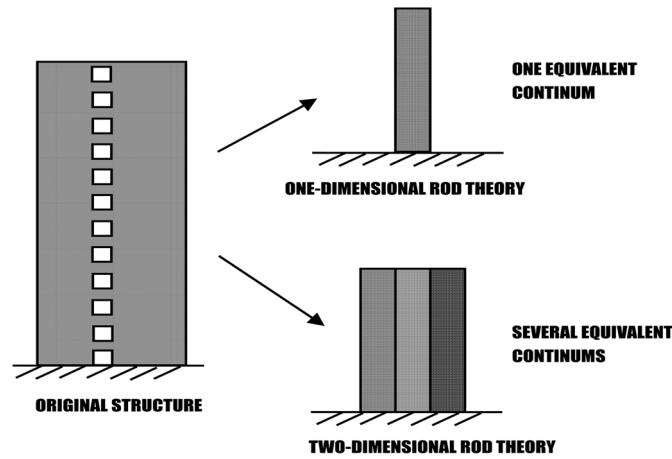


Fig. 1 The difference between one- and two-dimensional rod theories

shear-lag. The effectiveness of this theory was demonstrated by comparison with the numerical results obtained from a frame analysis on the basis of FEM code NASTRAN for various high-rise buildings, tube structures and mega structures. Also, Takabatake and Matsuoka(1983,1987) considered the local deformation and the distortion of the cross section in order to extend the coverage of the rod theory.

The equivalent rod theory replaces the original structure by a model of one-dimensional rod with an equivalent stiffness distribution, appropriate with regard to the global behavior. Difficulty arises in this modeling due to the restricted number of freedom of the equivalent rod; local properties of each structural member cannot always be properly represented, which leads to significant discrepancy in some cases. The one-dimensional idealization is able to deal only with the distribution of stiffness and mass in the longitudinal direction, possibly with an account of the averaged effects of transverse stiffness variation. In common practice, however, structures are composed of a variety of members or structural parts, often including distinct constituents such as a frame-wall or coupled wall with opening. Overall behavior of such a structure is significantly affected by the local distribution of stiffness. In addition, the individual behavior of each structural member plays an important role from the standpoint of structural design. It is the main objective of this paper to propose two-dimensional rod approximation as an extension of the one-dimensional rod theory to take into account of the effect of transverse variations in individual member stiffness.

Fig. 1 illustrates the difference between the one- and two-dimensional rod theories in evaluating the local stiffness distribution of structural components. In the two dimensional approximation, structural components with different stiffness and mass distribution are continuously connected. On the basis of linear elasticity, governing equations are derived from Hamilton's principle. Use is made of a displacement function which satisfies continuity conditions across the boundary surfaces between the structural components. Examples are considered for elastic building structures with numerical results obtained through finite difference scheme. Validity of the proposed approximation is confirmed with regard to static, free vibration and forced vibration problems by comparison with the results of shell-element based FEM code NASTRAN. Comparison is also made for the static solution by Smith and Coull (1991), in particular, for a uniform coupled wall with opening, leading to close agreement.

## 2. Governing equation

For the sake of simplicity, we consider the two-dimensional structure of which the stiffness varies in the transverse and longitudinal directions. A Cartesian coordinate system  $x, y, z$  as shown in Fig. 2 is employed, in which the axis  $x$  denotes the longitudinal axis, and the  $y$  and  $z$  the transverse axes. The coordinate axis  $x$  can be selected arbitrarily. For simplicity, the  $x$  axis is taken position in the left edge. Let us consider the structure composed of several structural parts with different stiffness. Each structural part is assumed to be parallel to the longitudinal axis  $x$  and to be homogeneous continuum in the transverse and longitudinal directions, respectively, in the cross section at a prescribed value of the longitudinal axis  $x$ . Also, each structural part connects continuously with the adjacent structural parts and satisfies the continuous condition for displacement. The number of the structural parts indicates ①, ②, ... in turn from the left hand side in the transverse direction. In order to assist the transverse axis  $y$ , each structural part has each local transverse axis  $y_i$  ( $i = 1, 2, 3, \dots, n$ ) which each original point is the left side of each structural part, as shown in Fig. 2(b).

The displacement components  $\frac{(i)}{U}(x, y, z, t)$ ,  $\frac{(i)}{V}(x, y, z, t)$ ,  $\frac{(i)}{W}(x, y, z, t)$  in the  $x$ -,  $y$ - and  $z$ -directions on the  $i$ -th structural part are expressed as

$$\frac{(i)}{U}(x, y, z, t) = u(x, t) - \sum_{k=1}^i y_k \phi_k(x, t) \quad (1)$$

$$\frac{(i)}{V}(x, y, z, t) = v(x, t) \quad (2)$$

$$\frac{(i)}{W}(x, y, z, t) = 0 \quad (3)$$

in which  $u(x, t)$  and  $v(x, t)$  are the longitudinal and transverse displacement components in the  $x$ - and  $y$ -directions on the axial point, respectively;  $\phi_k(x, t)$  is the rotational angle along the  $z$ -axis for the  $i$ -th structural part. The positive of these displacements takes for the positive value of the coordinate axis and the positive of the rotational angle  $\phi_k(x, t)$  takes for the clock wise along the positive  $z$ -axis, as shown in Fig. 3. In Eq. (1) the following summation rule to simplify the expression is used for the  $i$ -th structural part

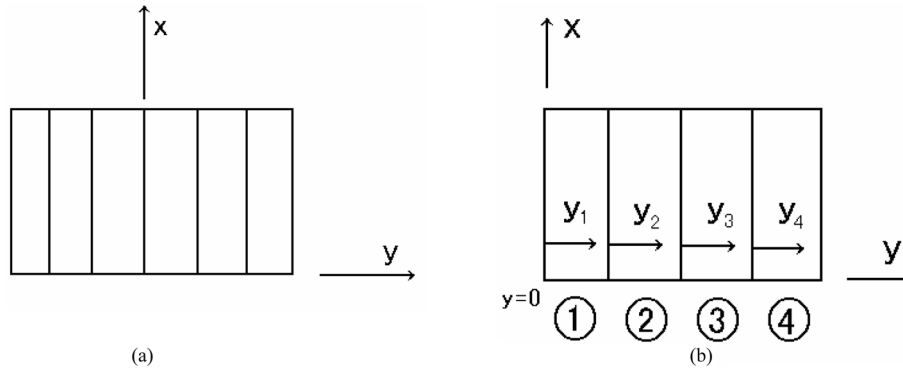


Fig. 2 Cartesian coordinate (a) global coordinate system, (b) local coordinate system

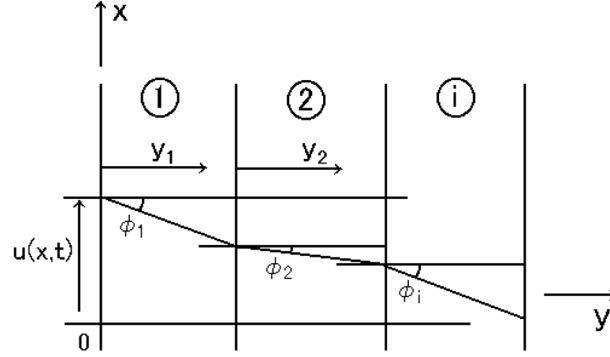


Fig. 3 Displacements and rotational angles

$$\sum_{k=1}^i y_k \phi_k = \sum_{k=1}^{i-1} \bar{y}_k \phi_k + y_i \phi_i \quad (4)$$

in which  $\bar{y}_k$  indicates the width of the  $k$ -th structural part.

Using the linear strain-displacement relation, the following expressions for the  $i$ -th structural part are obtained as

$$\varepsilon_x^{(i)} = \frac{\partial \bar{U}}{\partial x} = u' - \sum_{k=1}^i y_k \phi_k' \quad (5)$$

$$\gamma_{xy}^{(i)} = \frac{\partial \bar{U}}{\partial y_i} + \frac{\partial \bar{V}}{\partial x} = -\phi_i + v' \quad (6)$$

$$\gamma_{xz}^{(i)} = \frac{\partial \bar{U}}{\partial z} + \frac{\partial \bar{W}}{\partial x} = 0 \quad (7)$$

in which primes indicate the differentiation with respect to  $x$ ;  $\varepsilon_x^{(i)}$  and  $\gamma_{xy}^{(i)}$  are longitudinal and shear strains on the  $i$ -th structural part, respectively.

Employing the well-known engineering stress-strain relationship, the stresses on the  $i$ -th structural part are written as

$$\sigma_x^{(i)} = E^{(i)} \varepsilon_x^{(i)} \quad (8)$$

$$\tau_{xy}^{(i)} = \kappa G^{(i)} \gamma_{xy}^{(i)} \quad (9)$$

in which  $E^{(i)}$  and  $G^{(i)}$  are the Young modulus and shear modulus on the  $i$ -th structural part;  $\kappa$  is the shear coefficient.

Assuming the linear stress-strain relation, the strain energy,  $U$ , is given by

$$U = \frac{1}{2} \int_0^l [EA(u')^2 - 2u'(ES)_k \phi'_k + (EI)_{kj} \phi'_k \phi'_j + (\kappa GA)_k \phi_k^2 - 2(\kappa GA)_k \phi_k v' + \kappa GA(v')^2] dx \quad (10)$$

in which the summation rule for subscript is used as follows: for example for subscript  $k$

$$(\kappa GA)_k \phi_k^2 = (\kappa GA)_1 \phi_1^2 + (\kappa GA)_2 \phi_2^2 + \dots + (\kappa GA)_n \phi_n^2 \quad (11)$$

The sectional stiffnesses between structural parts may vary discontinuously with respect to  $x$  and  $y$ , respectively. The sectional stiffnesses for each structural part being homogeneous continuum with equivalent uniform thickness are defined as

$$\begin{aligned} A^{(i)} &= \iint dy_i dz \\ S_k^{(i)} &= \iint y_k dy_i dz \\ I_{kj}^{(i)} &= \iint y_k y_j dy_i dz \end{aligned} \quad (12)$$

in which  $A^{(i)}$ ,  $S_k^{(i)}$  and  $I_{kj}^{(i)}$  are the cross sectional area, the first and second inertia moments of the  $i$ -th structural part, respectively. In order to show concisely the sum of these sectional stiffness, we use the following notations in Eq. (10)

$$EA = \sum_{i=1}^n E A = E^{(1)(1)} A + E^{(2)(2)} A + \dots + E^{(n)(n)} A \quad (13)$$

$$(ES)_k = \sum_{i=k}^n E S_k^{(i)} \quad (14)$$

$$(EI)_{kj} = \sum_{i=\max(k,j)}^n E I_{kj}^{(i)} \quad (15)$$

$$(\kappa GA)_i = \kappa G A^{(i)} \quad (16)$$

$$\kappa GA = \sum_{i=1}^n \kappa G A^{(i)} \quad (17)$$

in which the subscript  $i=\max(k,j)$  of  $\sum$  in Eq. (15) indicates that the integral  $i$  takes the maximum of  $k$  and  $j$ .

The variation of the potential energy for current problem becomes

$$\delta V = - \int_0^l \{ [P_x - C_u \dot{u}] \delta u + (M)_k \delta \phi_k + [P_y - C_v \dot{v}] \delta v \} dx - [\tilde{P}_x \delta u + \tilde{P}_y \delta v + (\tilde{m})_k \delta \phi_k]_0^l \quad (18)$$

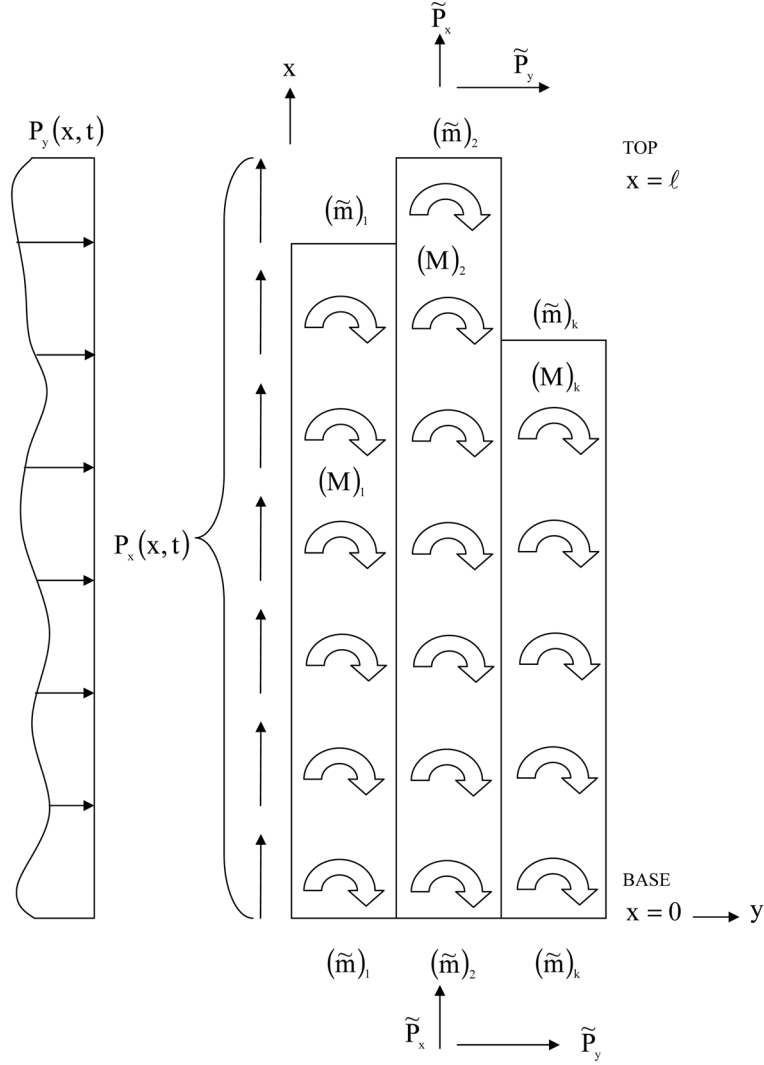


Fig. 4 External forces and external surface forces

in which  $P_x$  and  $P_y$  are components of external loads in the  $x$ - and  $y$ -directions per unit length, respectively; and  $(M)_k$  is the component of moment around the  $z$ -axis per unit length;  $C_u$  and  $C_v$  are damping coefficients of two-dimensional rod. Also,  $\tilde{P}_x$  and  $\tilde{P}_y$  are external surface forces in the  $x$ - and  $y$ -directions at the top ( $x=l$ ), respectively, and  $\tilde{m}_k$  is surface moment at the same point on the  $k$ -th structural part. The positive of these external forces is taken as shown in Fig. 4.

The current kinematic energy,  $T$ , defined as

$$T = \frac{1}{2} \iiint \rho \left[ \left( \frac{\dot{u}}{U} \right)^2 + \left( \frac{\dot{v}}{V} \right)^2 \right] dx dy dz \quad (19)$$

is written as

$$T = \frac{1}{2} \int_0^l [m(\dot{u})^2 - 2(\rho S)_k \dot{\phi}_k \dot{u} + (\rho I)_{kj} \dot{\phi}_k \dot{\phi}_j + m(\dot{v})^2] dx \quad (20)$$

in which the dot indicates differentiation with respect to time and  $\rho$  is mass density and  $m$  is mass per unit length as defined as

$$m = \sum_{i=1}^n \frac{(i)(i)}{\rho A} \quad (21)$$

Also,  $(\rho S)_k$  and  $(\rho I)_{kj}$  are defined as

$$(\rho S)_k = \sum_{i=1}^n \frac{(i)(i)}{\rho} S_k \quad (22)$$

$$(\rho I)_{kj} = \sum_{i=1}^n \sum_{k=1}^i \sum_{j=1}^i \frac{(i)(i)}{\rho} I_{kj} \quad (23)$$

The governing equation of the two-dimensional rod theory is proposed by means of the following Hamilton's principle

$$\delta I = \delta \int_{t_1}^{t_2} (T - U - V) dt = 0 \quad (24)$$

in which  $\delta$  is the variational operator taken during the indicated time interval. Substituting Eqs. (10), (18) and (20) into Eq. (24), the equations of motion can be obtained

$$\delta u : m\ddot{u} - (\rho S)_j \ddot{\phi}_j - (EAu')' + [(ES)_j \phi_j']' + C_u \dot{u} - P_x = 0 \quad (25)$$

$$\delta v : m\ddot{v} - [(\kappa GA)v' - (\kappa GA)_j \phi_j']' + C_v \dot{v} - P_y = 0 \quad (26)$$

$$\delta \phi_k : -(\rho S)_k \ddot{u} + (\rho I)_{kj} \ddot{\phi}_j + [(ES)_k u']' - [(EI)_{jk} \phi_j']' - (\kappa GA)_k v' + (\kappa GA)_k \phi_j \delta_k^j - (M)_k = 0 \quad (27)$$

together with the associated boundary conditions

$$\delta u : EAu' - (ES)_j \phi_j' = \tilde{P}_x \quad \text{or} \quad u = 0 \quad (28)$$

$$\delta v : (\kappa GA)v' - (\kappa GA)_j \phi_j' = \tilde{P}_y \quad \text{or} \quad v = 0 \quad (29)$$

$$\delta \phi_k : -(ES)_k u' - (EI)_{jk} \phi_j' = (\tilde{m})_k \quad \text{or} \quad \phi_k = 0 \quad (\text{for } k = 1, 2, 3 \dots n) \quad (30)$$

in which  $\delta_k^j$  is Kronecker delta. The theory proposed here is also applicable to a complicated problem included the setback and is considerable to the variation of both the longitudinal and transverse stiffnesses, as shown in Fig. 5. When the structure is composed of three structural parts in the transverse stiffness, the three rotational angles,  $\phi_1$ ,  $\phi_2$ ,  $\phi_3$ , corresponding to three structural parts, are prepared at least. The boundary conditions are applied to Eq. (30)<sub>1</sub> for  $\phi_1$  at the setback point I

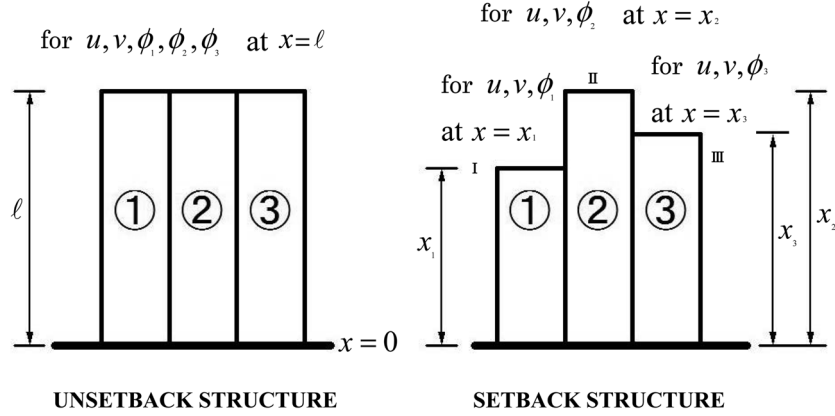


Fig. 5 Illustration of boundary point

at  $x=x_1$ , Eq. (30)<sub>1</sub> for  $\phi_3$  at the setback point III at  $x=x_3$ , and Eq. (28)<sub>1</sub>, (29)<sub>1</sub> and (30)<sub>1</sub> for  $u$ ,  $v$ , and  $\phi_2$  at the top at  $x=x_2$ , respectively.

If the structure has uniform stiffness in the transverse direction but variable stiffness in the longitudinal direction and has not discontinuous variation such as setback, the behavior of the structure can be treated with one structural part only. This implies that the distribution of the stress and strain in the cross section is linear in the transverse direction, as used in the well-known beam theory. The current governing equation with one structural part reduces to the Timoshenko beam theory. However, if the uniform beam has a discontinuous variation such as setback, the distribution of stress around the discontinuous stiffness is not linear and very complex. For such a case we can treat by preparing many structural parts to take account of the higher order deformation.

### 3. Free vibration

We consider to apply the free vibration problem to the two-dimensional rod theory. The method of separation of variables is employed assuming that

$$u(x, t) = \bar{u}(x)e^{i\omega t} \quad (31)$$

$$v(x, t) = \bar{v}(x)e^{i\omega t} \quad (32)$$

$$\phi_k(x, t) = \bar{\phi}_k(x)e^{i\omega t} \quad (33)$$

in which  $\bar{u}(x)$ ,  $\bar{v}(x)$ ,  $\bar{\phi}_k(x)$  are functions of  $x$ . Appending Eqs. (31)-(33) to the equation for free vibrations obtained from Eqs. (25)-(27), we have

$$-(EA)' \bar{u}' - EA \bar{u}'' (ES)_j \bar{\phi}_j' + (ES)_j \bar{\phi}_j'' - \omega^2 [m \bar{u} - (\rho S)_j \bar{\phi}_j] = 0 \quad (34)$$

$$-[(\kappa GA)' \bar{v}' + (\kappa GA) \bar{v}'' - (\kappa GA)_j \bar{\phi}_j' - (\kappa GA)_j \bar{\phi}_j''] - \omega^2 m \bar{v} = 0 \quad (35)$$

$$(ES)'_k \bar{u}' + (ES)_k \bar{u}'' - (EI)'_{jk} \bar{\phi}'_j - (EI)_{jk} \bar{\phi}''_j - (\kappa GA)_k \bar{v}' + (\kappa GA)_j \bar{\phi}_j \delta_k^j - \omega^2 [-(\rho S)_k \bar{u} + (\rho I)_{jk} \bar{\phi}_j] = 0 \quad (36)$$

The natural frequencies are obtained from eigen value problem of Eqs. (34) to (36) together with the associated boundary conditions.

#### 4. Forced vibration

If the natural frequencies and eigen values corresponding to a few natural modes for the longitudinal and transverse free vibrations are obtained, the forced vibration under elastic behaviors can be solved simply by means of the modal analysis. As for another method we can use the well-known step by the step integration method based on constant acceleration method (for example Buchholdt(1997)). This method is also applicable to inelastic problems. The increments of displacements and external loads during the time increment  $\Delta t$  from the time  $t$  are indicated by  $\Delta u(x,t)$ ,  $\Delta v(x,t)$ ,  $\Delta \phi_j(x,t)$ ,  $\Delta P_x$ ,  $\Delta P_y$ ,  $\Delta M_k$ ,  $\Delta \tilde{P}_x$ ,  $\Delta \tilde{P}_y$ ,  $\Delta \tilde{m}_k$  respectively. Thus, the incremental equations of motion using the constant acceleration method becofine

$$\begin{aligned} \delta \Delta u: \quad m \left( \frac{4}{\Delta t^2} \Delta u - \frac{4}{\Delta t} \dot{u} - 2\ddot{u} \right) - (\rho S)_j \left( \frac{4}{\Delta t^2} \Delta \phi_j - \frac{4}{\Delta t} \dot{\phi}_j - 2\ddot{\phi}_j \right) - (EA \Delta u)' + [(ES)_j \Delta \phi_j]' \\ + C_u \left( \frac{2}{\Delta t} \Delta u - 2\dot{u} \right) - \Delta P_x = 0 \end{aligned} \quad (37)$$

$$\delta \Delta v: \quad m \left( \frac{4}{\Delta t^2} \Delta v - \frac{4}{\Delta t} \dot{v} - 2\ddot{v} \right) - [(\kappa GA) \Delta v' - (\kappa GA)_j \Delta \phi_j]' + C_v \left( \frac{2}{\Delta t} \Delta v - 2\dot{v} \right) - \Delta P_y = 0 \quad (38)$$

$$\begin{aligned} \delta \Delta \phi_k: \quad -(\rho S)_k \left( \frac{4}{\Delta t^2} \Delta u - \frac{4}{\Delta t} \dot{u} - 2\ddot{u} \right) + (\rho I)_{kj} \left( \frac{4}{\Delta t^2} \Delta \phi_j - \frac{4}{\Delta t} \dot{\phi}_j - 2\ddot{\phi}_j \right) + [(ES)_k \Delta u]' \\ - [(EI)_{jk} \Delta \phi_j]' - (\kappa GA)_k \Delta v' + (\kappa GA)_k \Delta \phi_j \delta_k^j - \Delta (M)_k = 0 \end{aligned} \quad (39)$$

Solving the above equations for  $\Delta u(x,t)$ ,  $\Delta v(x,t)$ , and  $\Delta \phi_j(x,t)$  under the subjected boundary conditions, the incremental accelerations and velocities during the incremental time  $\Delta t$  are given by

$$\begin{Bmatrix} \Delta \ddot{u} \\ \Delta \ddot{v} \\ \Delta \ddot{\phi}_j \end{Bmatrix} = \frac{4}{\Delta t^2} \begin{Bmatrix} \Delta u \\ \Delta v \\ \Delta \phi_j \end{Bmatrix} - \frac{4}{\Delta t} \begin{Bmatrix} \dot{u}(t) \\ \dot{v}(t) \\ \dot{\phi}_j(t) \end{Bmatrix} - 2 \begin{Bmatrix} \ddot{u}(t) \\ \ddot{v}(t) \\ \ddot{\phi}_j(t) \end{Bmatrix} \quad (40)$$

$$\begin{Bmatrix} \Delta \dot{u} \\ \Delta \dot{v} \\ \Delta \dot{\phi}_j \end{Bmatrix} = \frac{2}{\Delta t} \begin{Bmatrix} \Delta u \\ \Delta v \\ \Delta \phi_j \end{Bmatrix} - 2 \begin{Bmatrix} \dot{u}(t) \\ \dot{v}(t) \\ \dot{\phi}_j(t) \end{Bmatrix} \quad (41)$$

Thus, we can calculate the time histories using the two-dimensional rod theory proposed by means of the step by step integrations.

## 5. Numerical calculation method

The two-dimensional rod theory replaces an original structure composed of various structural stiffnesses in the transverse direction with many continuous structural parts with uniform transverse stiffness. In this paper the numerical computation is considered to the shape of the structures without setback, but the stiffness is arbitrarily variable to the longitudinal and transverse directions. We use the finite difference method in the numerical computation. Since in the proposed theory the  $x$ -axis at an arbitrary point on the transverse cross section of the rod can be taken, the reduced equations of motion given by Eqs. (25)-(27) are in a coupled form.

Now, the boundary conditions are assumed to be clamped at the base and free at the top. Hence, from Eqs. (28)-(30)

$$u = 0 \quad (42)$$

$$v = 0 \quad (43)$$

$$\phi_k = 0 \quad (44)$$

at the base ( $x=0$ ) and

$$EAu' - (ES)_j \phi'_j = \tilde{P}_x \quad (45)$$

$$(\kappa GA)v' - (\kappa GA)_j \phi_j = \tilde{P}_y \quad (46)$$

$$-(ES)_k u' + (EI)_{jk} \phi'_j = (\tilde{m})_k \quad (\text{for } k = 1, \dots, n) \quad (47)$$

at the top ( $x = 1$ ).

## 6. Numerical results and discussions

The exactness of the two-dimensional rod theory proposed here is proven through a comparison of numerical results obtained from the proposed theory and FEM code NASTRAN for many numerical models. The calculation in FEM is obtained from applying usual shell elements to the original structures being the numerical models used herein. The mesh size of the shell elements is determined after confirming the convergence of numerical results. First, numerical results for a rod composed of structural parts which are variable in the longitudinal direction only agree with the ones obtained from the FEM code NASTRAN for static, free vibration, and forced vibration problems.

Next, we consider two dimensional rod composed of structural parts with different stiffness in both longitudinal and transverse directions, as shown in Fig. 6. This model is named as MODEL-0. Figs. 7(a) and 7(b) show the distribution of the lateral displacement and the bending moment subjected to static uniform lateral load 10 N/m, respectively. Figs. 8(a) and 8(b) present the natural modes and participation functions for transverse free vibrations, respectively. For forced vibration

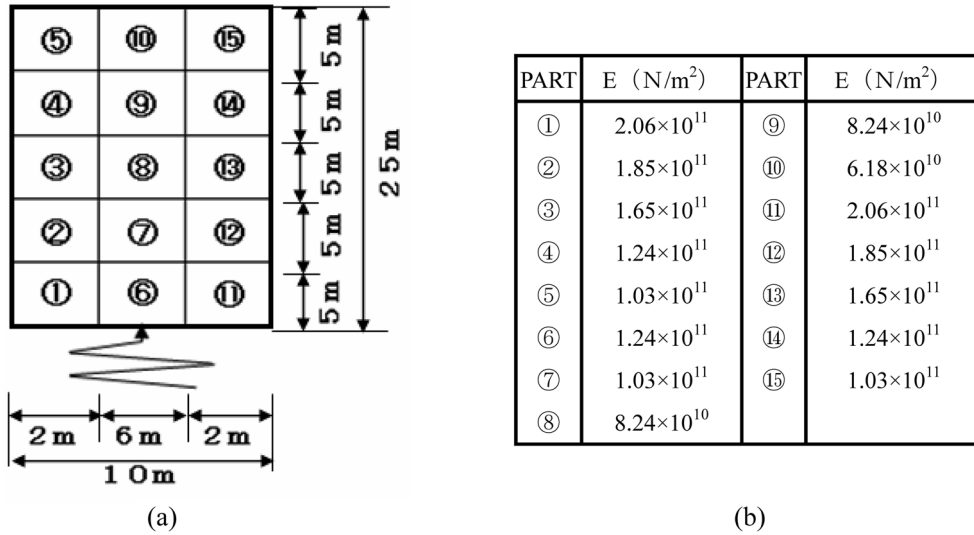


Fig. 6 MODEL-0 (a) size, (b) stiffness

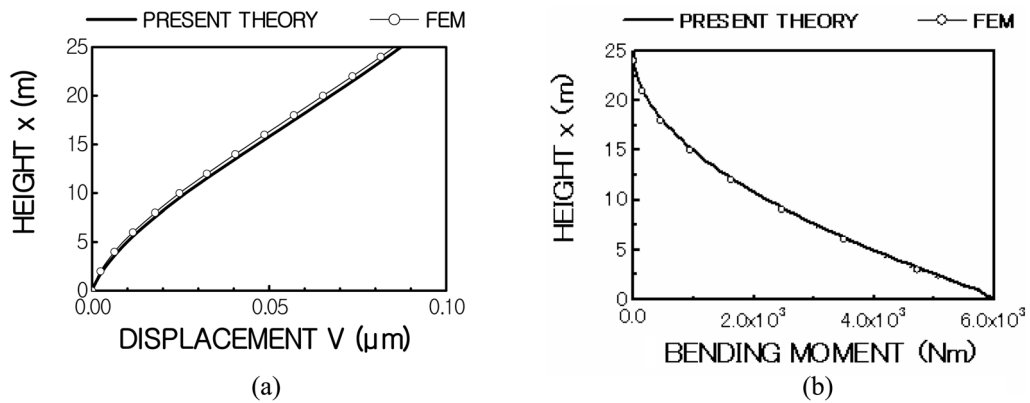


Fig. 7 Static numerical results of MODEL-0 (a) lateral displacement, (b) bending moment

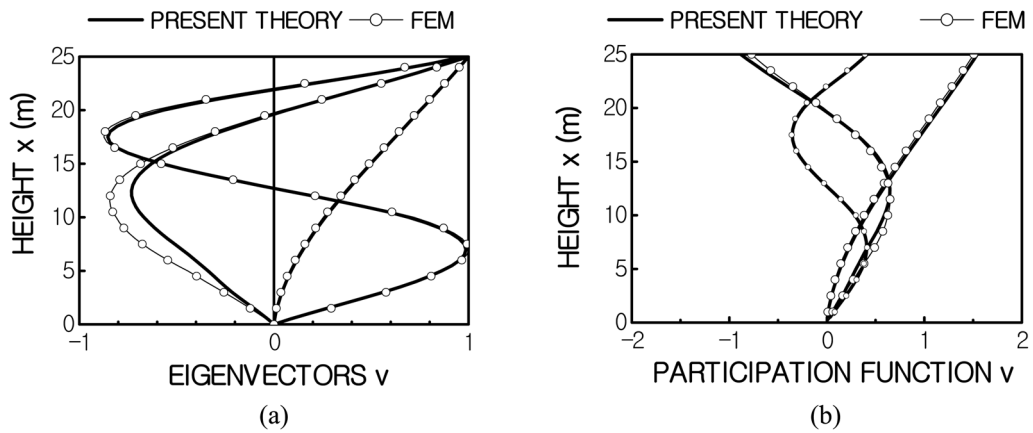


Fig. 8 Natural mode of MODEL-0 (a) lateral vibration, (b) participation function

subjected to earthquake waves at the base, the good agreement between analytical calculations and FEM code NASTRAN in the shell element is confirmed for the displacements, bending moments, and shear forces.

Next we consider the coupled shear wall structures with variable thickness to demonstrate the

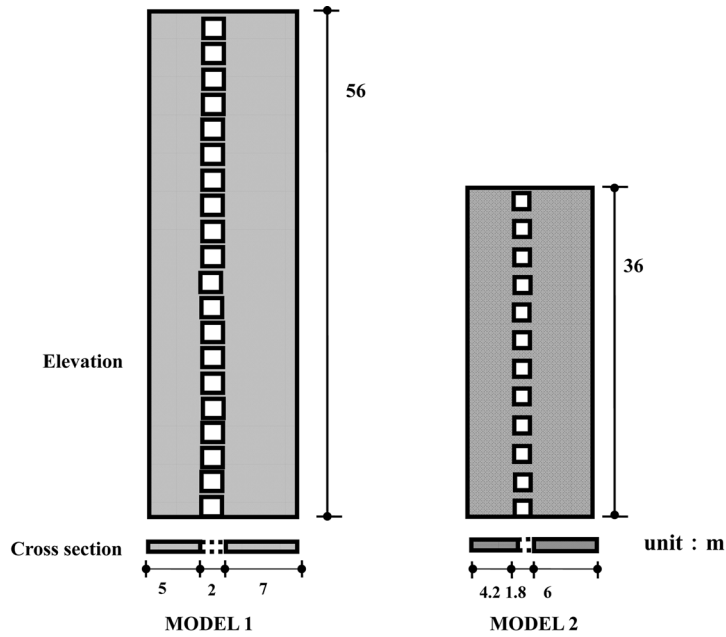


Fig. 9 MODEL-1 and MODEL-2

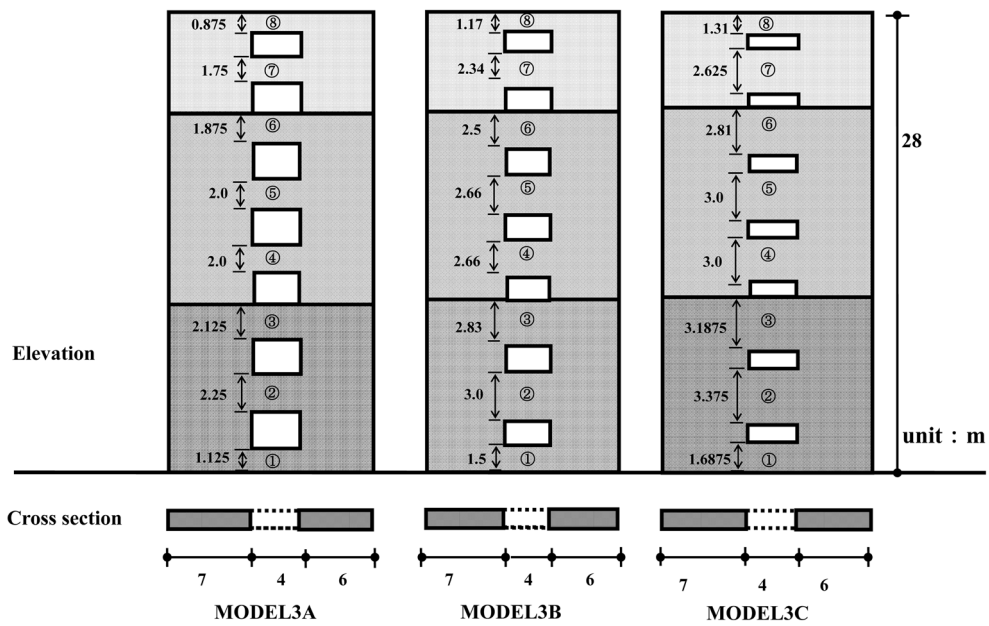


Fig. 10 MODEL-3A to 3C

Table 1 MODEL 1 , MODEL 2 and MODEL 3A-3C

		MODEL 1	MODEL 2	MODEL 3A-3C
Young Modulus $E$		$3.6 \times 10^{10}$ N/m <sup>2</sup>	$2.1 \times 10^{10}$ N/m <sup>2</sup>	$3.6 \times 10^{10}$ N/m <sup>2</sup>
Shear Modulus $G$		$1.565 \times 10^{10}$ N/m <sup>2</sup>	$9.14 \times 10^9$ N/m <sup>2</sup>	$1.565 \times 10^{10}$ N/m <sup>2</sup>
Mass Density $\rho$		$2.4 \times 10^3$ kg/m <sup>3</sup>	$2.4 \times 10^3$ kg/m <sup>3</sup>	$2.4 \times 10^3$ kg/m <sup>3</sup>
Poisson Ratio $\nu$		0.15	0.15	0.15
Damping Constant		0.05	0.05	0.05
Total Storeys		20	12	7
Total Height		56.0 m	36.0 m	28 m
Left Side Wall	Thickness	0.3 m	0.5 m	0.35 m, 0.3 m, 0.25 m
	Width	5.0 m	7.0 m	7.0 m
Right Side Wall	Thickness	0.3 m	0.5 m	0.35 m, 0.3 m, 0.25 m
	Width	7.0 m	6.0 m	6.0 m
	Width	0.3 m	0.5 m	0.35 m, 0.3 m, 0.25 m
Lintel	Height	0.4 m	0.45 m	1.5 m, 1.0 m, 0.8 m
	Length	2.0 m	1.8 m	4.0 m
Uniform Lateral Load		16.5 kN/m	10.0 kN/m	16.5 kN/m

effectiveness and distinction of the proposed two-dimensional rod theory. Smith and Coull(1991) presented the theory and design curves for practical method in the static problem of the coupled shear walls with uniform properties over the height. The analytical method can, by the judicious use of average properties, serve as a useful guide to the forces in nonuniform structures. Also Pübal(1988) has presented the analytical static method by simulating a wall with openings as systems of wall columns coupled by lintels having the function of members which substitute the cross-bars. The above-mentioned past methods are restricted in the static problem of uniform wall with openings. Five types of numerical models MODEL-1, MODEL-2, and MODEL-3A to -3C of reinforced shear walls are prepared, as shown in Figs. 9 and 10. Table 1 indicates numerical data for these models. MODEL-1 is an example of coupled shear wall structure used by Smith and Coull(1991). Model-2 is determined with the references of Pübal(1988) and Scarlet (1996). It has uniform thickness 0.3 m and a 20-story structure subjected to a uniformly distributed static load of intensity 16.5 kN/m. In the

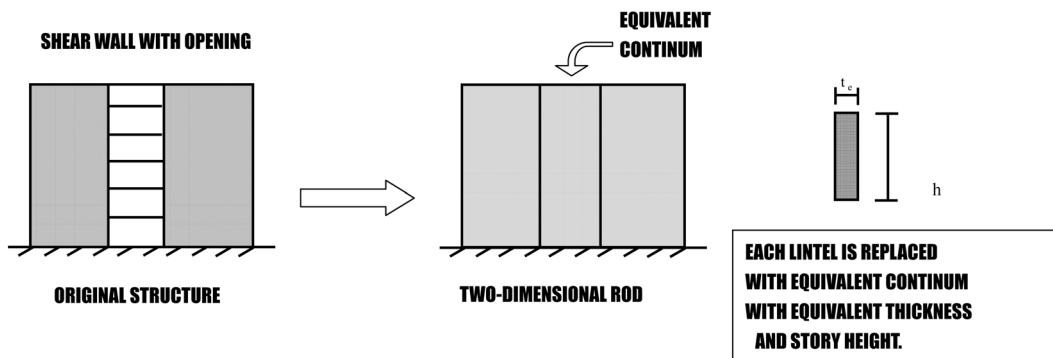


Fig. 11 Equivalent continuum with equivalent stiffness and mass

present two-dimensional rod theory the structural part composed of lintels is replaced with the continuous structural part having equivalent stiffness and mass, as illustrated in Fig. 11. The equivalent stiffness and mass of the structural part corresponding to a lintel are reflected on the equivalent thickness  $t_e$  and equivalent mass density  $\rho_e$ , respectively, given by

$$t_e = \frac{24(1 + \nu)I_b}{hl^2} \quad (48)$$

$$\rho_e = \rho \frac{t \bar{h}}{t_e h} \quad (49)$$

in which  $l$  is span-length of a lintel,  $h$  is a half height between the upper and lower lintels adjacent to current lintel, namely the story height. The notations  $\nu$ ,  $I_b$ ,  $t$ ,  $\bar{h}$ , and  $\rho$  are Poisson's ratio, moment of inertia, width, depth, and mass density of a lintel, respectively. Eq. (48) is proposed by Smith and Coull (1991) for the equivalent thickness. As for separate numerical approach to examine the numerical results, we prepare the numerical computation applied shell element on FEM code NASTRAN to the original coupled shear wall structure with opening, in which all shear walls and lintels are subdivided by a shell element. Fig. 12(a) shows the distribution of static displacements. It

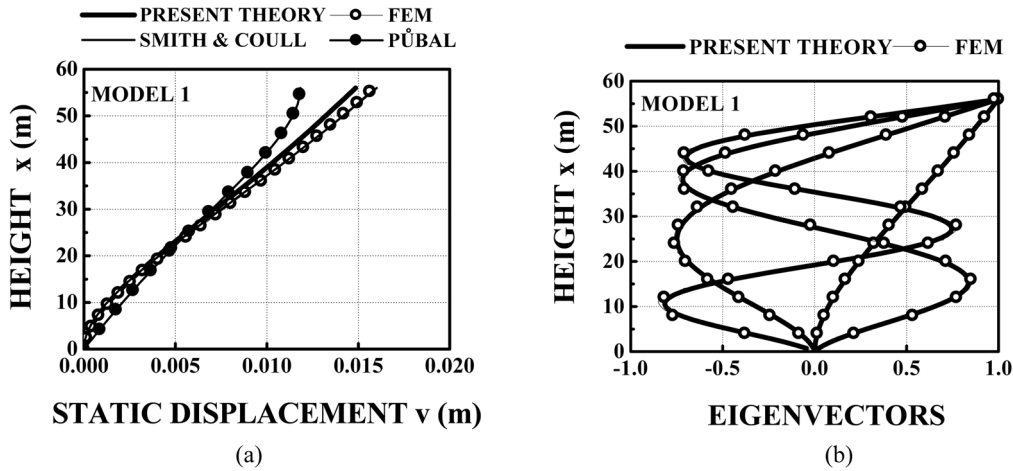


Fig. 12 Numerical result of MODEL-0 (a) static displacement, (b) natural mode of lateral free vibration

Table 2 Natural frequencies for lateral vibration

	MODEL1			MODEL2		
	PRESENT THEORY ①	FEM ②	RATIO ① / ②	PRESENT THEORY ①	FEM ②	RATIO ① / ②
1st mode	13.43	13.09	1.026	20.75	19.97	1.039
2nd mode	56.48	55.55	1.017	84.27	82.15	1.026
3rd mode	130.55	129.00	1.012	196.13	191.00	1.027
4th mode	227.16	224.90	1.010	320.93	313.64	1.023

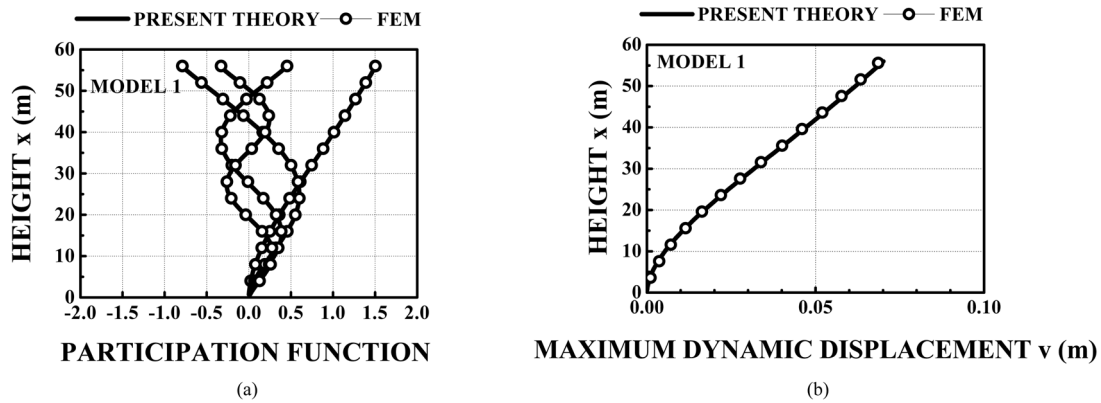


Fig. 13 Numerical result for lateral vibration of MODEL-1 (a) participation function, (b) maximum dynamic displacement

indicates the good agreement between Smith and Coull(1991) and FEM computational results. It shows that the numerical result obtained from the present theory proposed is slightly stiffer for deflection. The natural frequency and eigenfunction for free vibration and participation functions are shown in Table 2 and Figs. 12(b) and 13(a), respectively. The maximum dynamic response of the same structure subjected to earthquake wave EL Centro 1940-NS at the base shows a good agreement between the present theory and FEM, as shown in Fig. 13(b).

MODEL-2 is also the uniform thickness 0.5 m and the 12-story with the total height 36 m. The numerical results indicate the same behavior as MODEL-1 and demonstrates the good agreement between the present theory and NASTRAN.

The above-mentioned numerical results are based on numerical models for shear walls with the uniform thickness and relative large openings. Then in order to examine the exactness of the theory proposed here to common shear walls which the wall thickness and the size of openings vary in the height, MODEL-3A to MODEL-3C, as shown in Fig. 10, are prepared. These models vary both the wall thickness and openings with the three stages in the height direction. The size of openings of these models are smaller than MODEL-1 and MODEL-2. When the openings are large, the stiffness of lintel is small and the effect of rotation produced at the both ends of the lintel due to the rotation of the shear walls is negligible in the calculation of equivalent stiffness of structural part corresponding to lintel as given by Eq. (48). On the other side, when the size of openings such as the MODEL-3A to 3C is relatively small, the stiffness of a lintel has an influence on constrained condition at the both ends because both ends of the lintel is affected remarkably on the rotation of both shear walls which the lintels connect at the both ends. Numerical results used equivalent thickness obtained from Eq.(48) for structural parts composed of lintels indicate to be harder than one from FEM code NASTRAN in the deformation. A simplified design equation for the equivalent thickness included the effect of rotation at the both ends of the lintel due to the rotation of both shear walls is necessary instead of Eq.(48) to improve the accuracy of the present two-dimensional rod theory. As for the practical method to estimate equivalent thickness this paper proposes to replace the real span length  $l$  of a lintel with the more longer span length  $\bar{l}$  in Eq.(48) proposed by Smith and Coull(1991). The relationships between the replaced span length  $\bar{l}$  and real span length  $l$  is related as

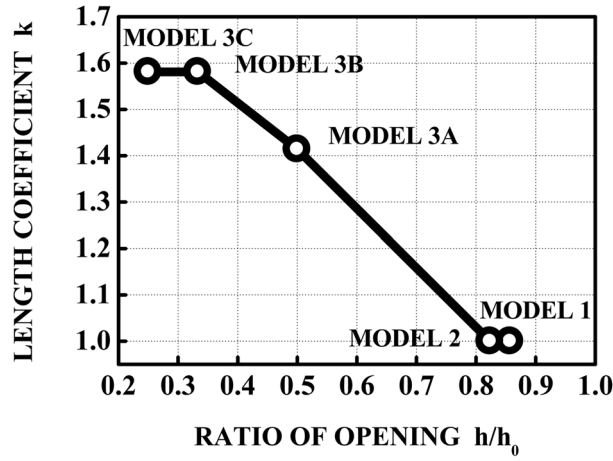


Fig. 14 Relationships between  $k$  and  $h/h_0$

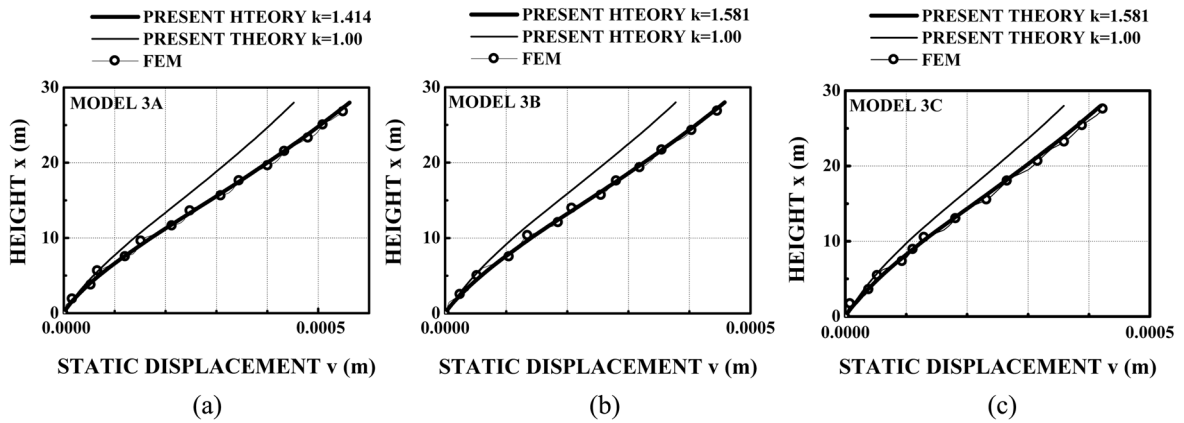


Fig. 15 Static lateral displacements (a) MODEL 3A, (b) MODEL 3B and (c) MODEL 3C

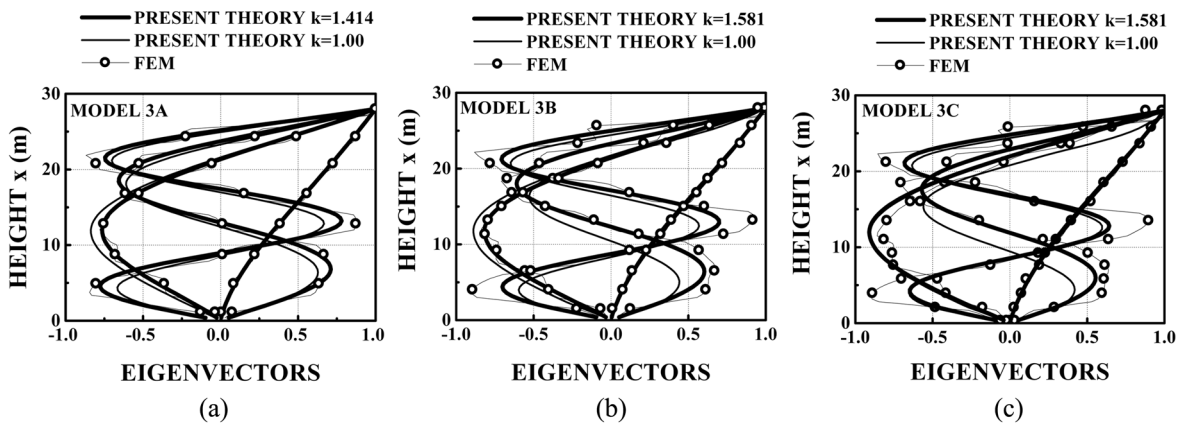


Fig. 16 Natural mode (a) MODEL 3A, (b) MODEL 3B and (c) MODEL 3C

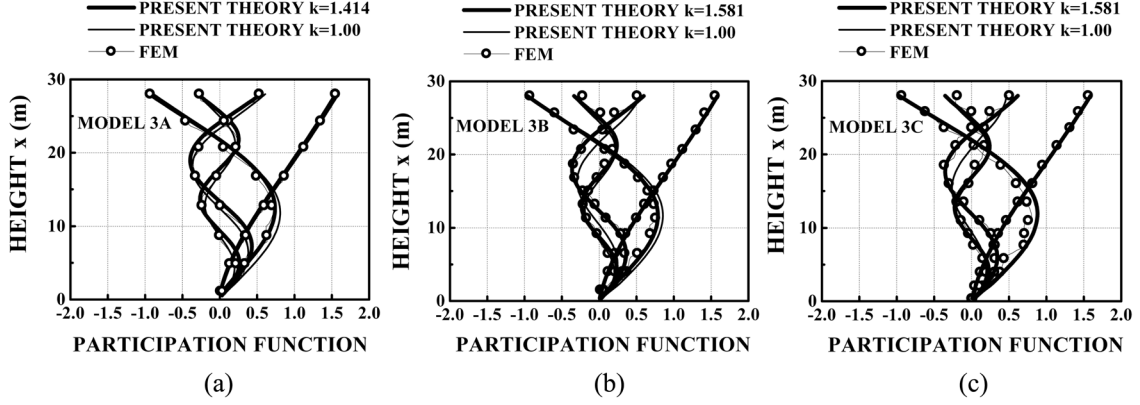


Fig. 17 Participation functions (a) MODEL 3A, (b) MODEL 3B and (c) MODEL 3C

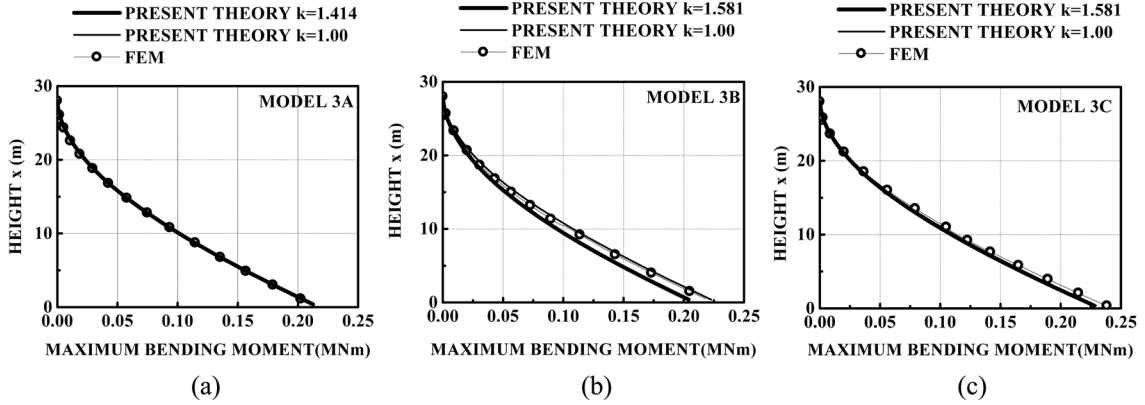


Fig. 18 Maximum bending moment (a) MODEL 3A, (b) MODEL 3B and (c) MODEL 3C

Table 3 Natural frequencies for lateral vibration

MODEL 3A	PRESENT THEORY ①	PRESENT THEORY K = 1.414 ②	FEM ③	RATIO	
				① / ③	① / ③
1st mode	70.841	63.987	64.307	1.102	0.995
2nd mode	224.428	207.437	207.819	1.080	0.998
3rd mode	466.356	423.655	423.993	1.100	0.999
4th mode	703.520	655.756	655.118	1.074	1.001

$$\bar{l} = kl \quad (57)$$

in which  $k$  is correction coefficient and depends on the height ratio of openings  $h/h_0$ , in which  $h_0$  is the height of the opening. Fig. 14 shows the relationships between  $k$  and  $h/h_0$ . These relationships are obtained by comparing the numerical results for all models in this paper with the results by FEM. Figs. 15, 16 and 17 show static lateral displacements, eigenvectors, participation functions for Model 3A to 3C, respectively. Fig. 18 indicates the distribution of maximum bending moment

subjected to earthquake wave at the base. The use of the correction coefficient  $k$  on the computation of the equivalent thickness  $t_e$  is shown to be effective to improve the accuracy of the numerical results except for natural frequencies because the effect of the stiffness of structure part composed of lintels is very small on the transverse and longitudinal free vibrations. Table 3 indicates that the effect of lintel's stiffness is very small in the natural frequencies of the transverse free vibration.

## 7. Conclusions

Two-dimensional rod theory has been presented for simply analyzing a large or complicated structure such as a high-rise building or shear wall with opening. The principle of this theory is that the original structure comprising various different structural components is replaced by an assembly of continuous strata which has stiffness equivalent to the original structure in terms of overall behavior. The two-dimensional rod theory is an extended version of a previously proposed one-dimensional rod theory for better approximation of the structural behavior. The effectiveness of this theory has been demonstrated from numerical results for exemplified building structures of distinct components. This theory may be applicable to soil-structure interaction problems involving the effect of multi-layered or non-uniform grounds.

## Acknowledgments

This research is supported by Grant-in-Aid for Scientific Research in Japan. The writer would like to express their appreciation to Y. Kawae and Y. Nomura, undergraduate students of Kanazawa Institute of Technology, for their help in computational programming.

## References

- Buchholdt, H. (1997), *Structural dynamics for engineers*, Thomas Telford.
- Georgoussis, G.K. (2006), "A simple model for assessing periods of vibration and modal response quantities in symmetrical buildings", *Struct. Des. Tall Spec. Build.*, **15**(2), 139-151.
- Pöbäl, Z. (1988), *Theory and calculation of frame structures with stiffening walls*, Elsevier, Amsterdam.
- Rutenberg, A. (1975), "Approximate natural frequencies for coupled shear walls", *Earthq. Eng. Struct. D.*, **4**(1), 95-100.
- Smith, B.S. and Coull, A. (1991), *Tall building structures: analysis and design*, John Wiley & Sons, New York.
- Scarlet, A.S. (1996), *Approximate methods in structural seismic design*, E&FN Spon.
- Takabatake, H. and Matsuoka, O. (1983), "The elastic theory of thin-walled open cross sections with local deformations", *Int. J. Solids Struct.*, **19**(12), 1065-1088.
- Takabatake, H., and Matsuoka, O. (1987), "Elastic analyses of circular cylindrical shells by rod theory including distortion of cross section", *Int. J. Solids Struct.*, **23**(6), 797-817.
- Takabatake, H., Mukai, H. and Hirano, T. (1993a), "Doubly symmetric tube structures: I: static analysis", *J. Struct. Eng-ASCE*, **119**(7), 1981-2001.
- Takabatake, H., Mukai, H. and Hirano, T. (1993b), "Doubly symmetric tube structures: II: dynamic analysis", *J. Struct. Eng-ASCE*, **119**(7), 2002-2016.
- Takabatake, H., Takesako, R. and Kobayashi, M. (1995), "A simplified analysis of doubly symmetric tube structures", *Struct. Des. Tall Spec. Build.*, **4**(2), 137-153.

- Takabatake, H. (1996), "A simplified analysis of doubly symmetric tube structures by the finite difference method", *Struct. Des. Tall Spec. Build.*, **5**(2), 111-128.
- Takabatake, H. and Nonaka, T. (2001), "Numerical study of Ashiyahama residential building damage in the Kobe Earthquake", *Earthq. Eng. Struct. D.*, **30**(6), 879-897.
- Takabatake, H., Nonaka, T. and Tanaki, T. (2005), "Numerical study of fracture propagating through column and brace of Ashiyahama residential building in Kobe Earthquake", *Struct. Des. Tall Spec. Build.*, **14**(2), 91-105.
- Takabatake, H. and Satoh, T. (2006), "A simplified analysis and vibration control to super-high-rise buildings", *Struct. Des. Tall Spec. Build.*, **15**(4), 363-390.
- Tarjian, G. and Kollar, L.P. (2004), "Approximate analysis of building structures with identical stories subjected to earthquake", *Int. J. Solids Struct.*, **41**(5), 1411-1433.